Investigations of the galaxies of the LCV

Dimitrios Papachistopoulos

March 23, 2023

1 The Galaxies in the Local Cosmological Volume (LCV)

The Catalogue of Neigbouring Galaxies (Karachentsev, Igor D. and Makarov et al. 2013[2]) and its updated version from the "Catalog & Atlas of the LV galaxies" databas[1] are used to extract the K-band luminosities, the types of the galaxie[1]s, the mass within the Holmberg radius (M26), the Hydrogen masses of the galaxies (M_{HI}) and the SFRs based on integrated H and far-ultraviolet (FUV) measurments for galaxies within a distance of ≈ 11 Mpc. The SFR and MHI values contain limit flags, which we exclude from our present analysis. This gives a sample of 793 galaxies from 1248. From the remaing galaxies we have

	0
Name	793
Kmag	321
FUVmag	687
TType	793
Tdw1	580
Tdw2	568
Bmag	790
SFR_Ha	566
SFR_FUV	688
K	789
MHI	643
color	321

[1]TType=Morphology type code according to the classification by de Vaucouleurs/ Tdw1=Dwarf galaxy morphology/ Tdw2=Dwarf galaxy surface brightness morphology

Measurment	Number of Galaxies

The K-band values are converted to the total Stellar Masses of each galaxy according to the mass-to-light ratio of 0.6 ([5]), and the M_{HI} can be converted to the total mass of the gas of the galaxy using the equation $M_g = 1.33\, M_{HI}$

The total SFR of each galaxy can be calcuated by

$$SFR_o = \frac{SFR_{FUV} + SFR_{Ha}}{2}$$

if both $SFR_{H\alpha}, SFR_{FUV}$ measurments are available. If only one only one of them is given, then the SFR is equal to the given SFR value

$$SFR_o = SFR_i,\ \text{if}\ SFR_j = 0, i \neq j,\ i,j = FUV, H_a$$

The condition $SFR_o \geq 10^{-3} M_{\odot} yr^{-1}$ leaves 579 galaxies. This condition is applied due to the reasons given in the P. Kroupa,M. Haslbauer, I. Banik, S. T. Nagesh and J. Pflamm-Altenburg et al. 2020 [4]

2 Types of galaxies

Using the dataset of 1248 galaxies, do before using the condition and removing the galaxies with the flags, the below histograms can be plotted.

Most of the galaxies in the LCV are Higly Irregular galaxies followed by lenticular galaxies

Out of the 1248 galaxies the 1022 are dwarf galaxies

Most dwarf galaxies have low brightness and are irregulars followed by Dwarf spheroidal.

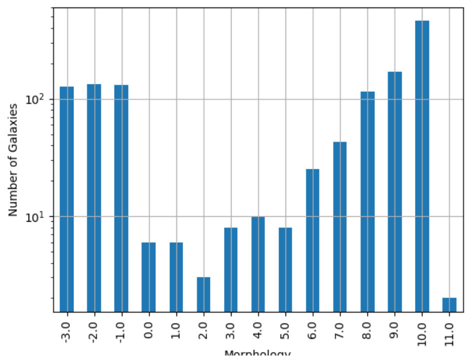

Figure 1: The classification by de Vaucouleurs et al. (1991) is used for the morphology of the galaxies

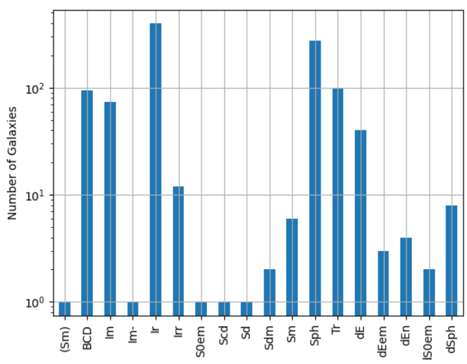

Figure 2: Dwarf galaxy morphology

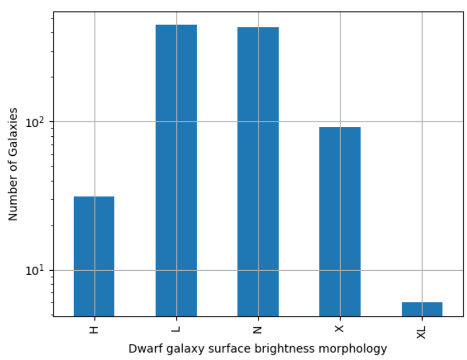

Figure 3: Dwarf galaxy surface brightness morphology, where: H = high; N = normal; L = low; X = extremely low.

3 Delayed-τ model

According to P. Kroupa et al. 2020[4] current star formation rates of galaxies can be described by the 'delayed-τ' mode as

$$SFR_{0,del} = \frac{A_{del} x e^{-x}}{\tau}, \text{ where } x = \frac{t_{sf}}{\tau} \quad (1)$$

where τ is the star formation time-scale, t_{sf} is the real time of star formation in a given galaxy and A_{del} a normalization constant.

The average SFR is

$$\overline{SFR}_{del} = \frac{A_{del}}{t_{sf}}[1 - (1 + x)e^{-x}] \quad (2)$$

and can also be defined by the present day stellar mass

$$\overline{SFR} = \frac{\zeta M_*}{t_{sf}} \quad (3)$$

where ζ accommodates for mass-loss through stella evolution and $\zeta \approx 1.3$

This is a system of 2 equations and 3 variables, since A_{del} has never been calculated

3.1 Constant t_{sf}

The observed ages of galactic discs are $t_{sf} \approx 12$ Gyr[3], so assuming an approximation of $t_{sf} = 12.5$ Gyr, the $\overline{SFR}_{del}$ can be calcuated, from the equation (**??**).

After that the equation of ratio

$$\frac{\overline{SFR}_{del}}{SFR_{0,del}} = \frac{e^x - x - 1}{x^2} \quad (4)$$

can be solved numerically for x and using the equations (**??**) and (**??**) the A_{del} and τ of each galaxy are found.

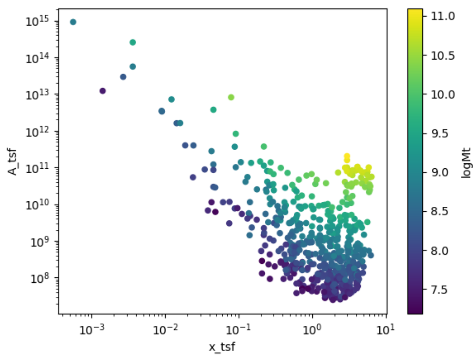

	A_tsf	tau	x_tsf
count	5.78E+02	5.79E+02	5.79E+02
mean	2.25E+12	1.09E+11	1.85E+00
std	3.94E+13	1.04E+12	1.48E+00
min	2.48E+07	1.93E+09	5.59E-04
25%	1.41E+08	4.18E+09	5.65E-01
50%	6.84E+08	7.79E+09	1.60E+00
75%	5.70E+09	2.21E+10	2.99E+00
max	9.10E+14	2.24E+13	6.47E+00

Figure 4: $A_{del} = f(x)$ for constant t_{sf}

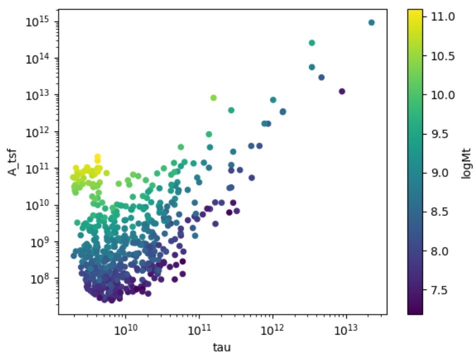

	A_tau	x_tau	tsf
count	5.79E+02	5.79E+02	5.79E+02
mean	4.59E+09	2.54E+00	8.89E+09
std	1.50E+10	9.57E-01	3.35E+09
min	9.87E+06	4.07E-01	1.42E+09
25%	6.50E+07	1.87E+00	6.55E+09
50%	2.37E+08	2.44E+00	8.54E+09
75%	1.12E+09	3.08E+00	1.08E+10
max	1.06E+11	5.77E+00	2.02E+10

3.2 Constant τ

Assuming for an constant $\tau = 3.5$ Gyr, we cannot use the same $\overline{SFR}$ since it depends on t_{sf}. Using the equations~(**??**) and (**??**)

$$\frac{\overline{SFR_{del}}}{SFR_{0,del}} = \frac{e^x - x - 1}{x^2} \Leftrightarrow \frac{e^x - x - 1}{x} = \frac{\zeta M_*}{SFR \cdot \tau}$$

using this equation x and A_{del} can be calculated numerically.

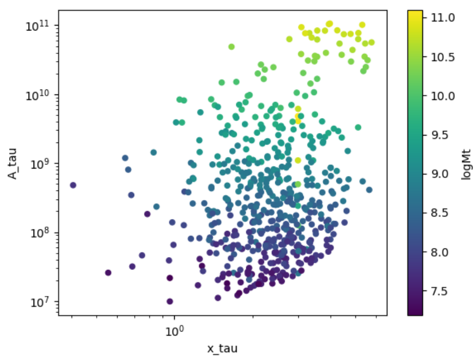

Figure 5: $A_{del} = f(x)$ for constant τ

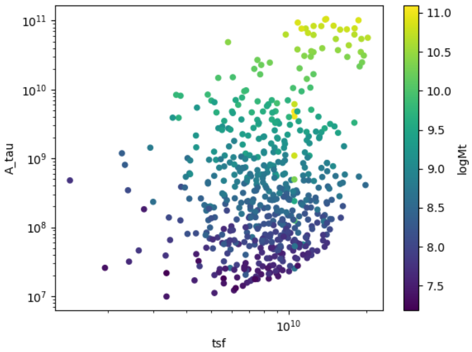

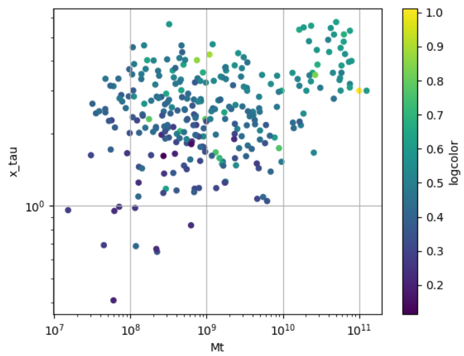

Figure 7: $x|_\tau = f(M_t)$, with their color index

3.3 Comparing the two results

3.3.1 Comparing the x's

Comparing the two different results for x, we see that the $x|_\tau$ has a lower σ

	x_tau	x_tsf
count	5.79E+02	5.79E+02
mean	2.54E+00	1.85E+00
std	9.57E-01	1.48E+00
min	4.07E-01	5.59E-04
25%	1.87E+00	5.65E-01
50%	2.44E+00	1.60E+00
75%	3.08E+00	2.99E+00
max	5.77E+00	6.47E+00

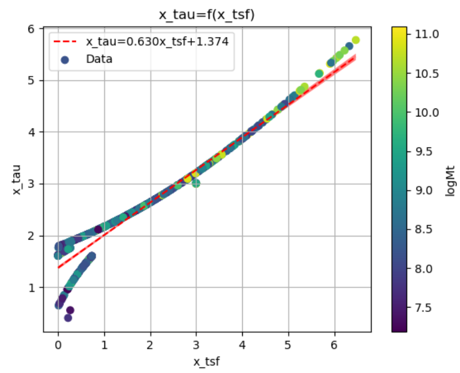

Figure 8: Comparing the two x, according to their total mass

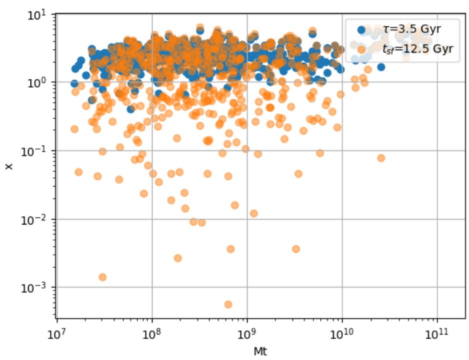

Figure 6: Comparing the two x's, According to their total masses

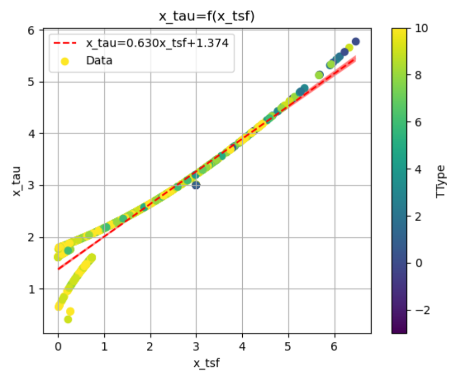

Figure 9: Comparing the two x, according to their type

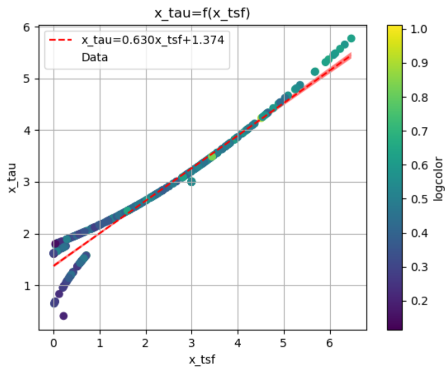

Figure 10: Comparing the two x, according to their color index

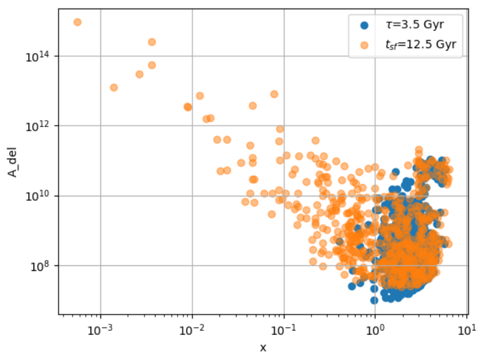

Figure 11: Comparing the two A_{del}

The two results are interrelated through the equation:

$$x|_\tau = (6.30(6) \times 10^{-1}) \cdot x|_{tsf} + (1.374(15) \times 10^0)$$
$$\text{with correlation } R^2 = 94\% \tag{5}$$

and from the plots the following conclusions can be drawn:

1. The galaxies with a higher total mass deviate less from the linear fit and are older.
2. The younger galaxies are mainly later types of galaxies
3. For lower x's, the galaxies have a lower color index which indicates that they are younger. So the values are inline with the experimental values.

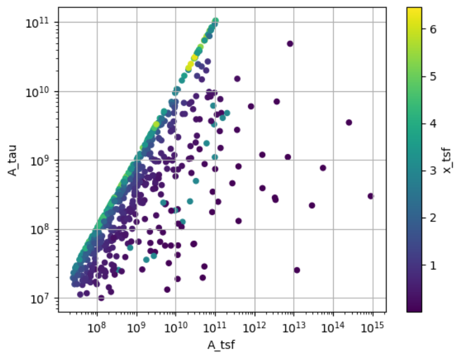

Figure 12: Comparison of the 2 A_{del}s according to their x

3.3.2 Comparing the normalization constants

For high x and high masses the two A_{del}s have a high correlation. Specifically:

1. For high x the $A_{del}|_\tau - A_{del}|_{t_{sf}}$ plot follows a $y = x$ trend, which means that for older stars and stars with a low star formation timescale τ, the normalization constant is the same despite the method used to calculate it.
2. The same is true for more massive galaxies, since they deviate less from the $y = x$ line

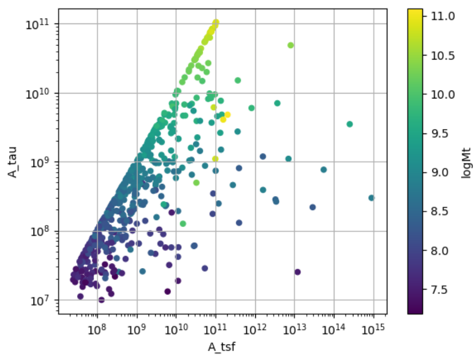

Figure 13: Comparison of the 2 A_{del}s according to their total masses

4 The gas depletion timescale τ_g

The gas depletion timescale τ_g measures the time taken by a galaxy to exhaust its gas content Mg given the current SFR[6, 7].

$$\tau_g = \frac{M_g}{\dot{M}_*} = \frac{M_g}{SFR}$$

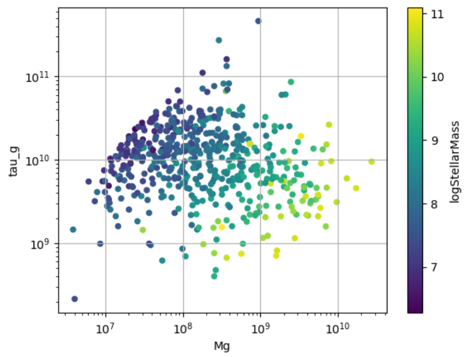

Figure 14: $\tau_g = f(M_g)$, with the Stellar Mass of the galaxies

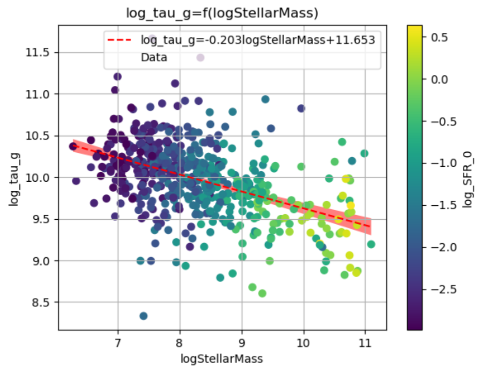

Figure 15: Correlation of the τ_g with the SFR and the Stellar mass

Even though the logarithmic correlation is low ($R^2 = 21\%$), there seems to be a pattern wherein the decrease of τ_g corresponds to an increase in the values of the Stellar Mass and the current star formation SFR_0.

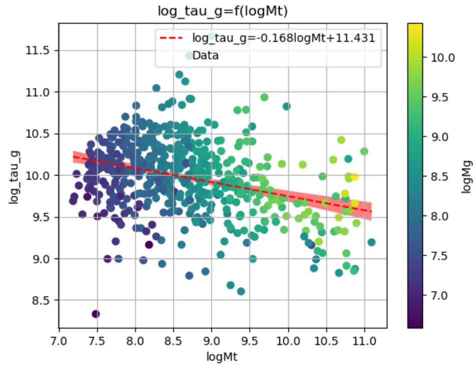

Figure 16: Correlation of the τ_g with the total mass and the mass of the gas

Again it can be observed that as the τ_g decreases, the corresponding values of M_t and M_g increase, but the logarithmic correlation is again low ($R^2 = 11\%$).

There is a notable trend, wherein for high masses we have a shorter timescale

5 Mass relations

Many of the galaxies masses have a high correlation with each other, and also help us undarstand the previous calculations.

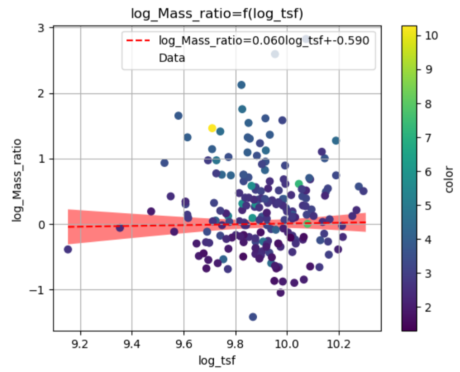

Figure 17: None

As expected, the older the galaxy the mass ratio is higher, and the color index agrees (\?)

References

[1] *Catalog of the LV Galaxies*. https://www.sao.ru/lv/lvgdb/tables.php. (Visited on 03/13/2023).

[2] Igor D. Karachentsev, Dmitry I. Makarov, and Elena I. Kaisina. “UPDATED NEARBY GALAXY CATALOG”. In: *AJ* 145.4 (Mar. 2013), p. 101. ISSN: 0004-6256, 1538-3881. DOI: 10.1088/0004-6256/145/4/101. (Visited on 03/13/2023).

[3] R. A. Knox, M. R. S. Hawkins, and N. C. Hambly. “A Survey for Cool White Dwarfs and the Age of the Galactic Disc”. In: *Monthly Notices of the Royal Astronomical Society* 306.3 (July 1999), pp. 736–752. ISSN: 0035-8711. DOI: 10.1046/j.1365-8711.1999.02625.x. (Visited on 03/13/2023).

[4] P Kroupa et al. “Constraints on the Star Formation Histories of Galaxies in the Local Cosmological Volume”. In: *Monthly Notices of the Royal Astronomical Society* 497.1 (Sept. 2020), pp. 37–43. ISSN: 0035-8711. DOI: 10.1093/mnras/staa1851. (Visited on 03/13/2023).

[5] Federico Lelli, Stacy S. McGaugh, and James M. Schombert. “SPARC: MASS MODELS FOR 175 DISK GALAXIES WITH SPITZER PHOTOMETRY AND ACCURATE ROTATION CURVES”. In: *AJ* 152.6 (Nov. 2016), p. 157. ISSN: 1538-3881. DOI: 10.3847/0004-6256/152/6/157. (Visited on 03/13/2023).

[6] Srikanth T. Nagesh et al. “Simulations of Star-Forming Main-Sequence Galaxies in Milgromian Gravity”. In: *Monthly Notices of the Royal Astronomical Society* 519 (Mar. 2023), pp. 5128–5148. ISSN: 0035-8711. DOI: 10.1093/mnras/stac3645. (Visited on 03/13/2023).

[7] Jan Pflamm-Altenburg and Pavel Kroupa. “The Fundamental Gas Depletion and Stellar-Mass Buildup Times of Star Forming Galaxies”. In: *ApJ* 706.1 (Nov. 2009). Comment: accepted for publication in ApJ, pp. 516–524. ISSN: 0004-637X, 1538-4357. DOI: 10.1088/0004-637X/706/1/516. arXiv: 0910.1089 [astro-ph]. (Visited on 03/22/2023).